Optimizing design of 3D seismic acquisition by CRS trace interpolation

Soleimani, M.[1*] and Roshandel Kahoo, A.[1]

1. Assistant Professor, Faculty of Mining, Petroleum and Geophysics, Shahrood University of Technology, Shahrood, Iran

Abstract

Land seismic data acquisition in most practical cases suffers from obstacles in fields which deviates geometry of the real acquired data from what was designed. These obstacles will cause gaps, narrow azimuth and offset limitation in the data. These shortcomings, not only prevents regular trace distribution in bins, but also distorts the subsurface image by reducing illumination of the target formation. However, some methods available can compensate the gaps in data due to field obstacles mainly by trace interpolation techniques. The common reflection surface (CRS) method that was previously introduced for seismic imaging in complex geological structures also could be used for trace interpolation to fill the gaps and to increase the fold of the data. In this study, we combined two different methods of trace interpolation and distribution in bins for solving the problem of gaps and low illumination of the target formation in a 3D seismic acquisition study area in the southwest of Iran. After processing old 2D lines available from the same area, the CRS parameters were obtained for proper definition of the acquisition design. Then by combining the CRS trace interpolation scheme and trace distribution, possible gaps in the data was resolved and regular trace distribution in all bins and azimuths were achieved. Result showed increasing redundancy in bins, which will prevent occurring gaps in data in case of inevitable field obstacles. Result shows that this strategy could be used to construct lost traces and prevent further problem in seismic imaging.

1. Introduction

Increasing density and/or reduce sparseness of three dimensional (3D) spatially sampling land seismic data is always a concern in any seismic acquisition design. In any 3D acquisition plane, the most important goal is to increase coverage of the subsurface target illumination (Chen et al., 2016). This goal is achieved by narrow shot and receiver line interval and low rolling number. However, regular trace distribution in offset and azimuth and appropriate sampling of the seismic wave-field with high fold should be considered for an optimized acquisition design (Kim et al., 2015). Harsh topography with station points, difficult to access, governmental restrictions, natural and manmade obstacles and social problems will also introduce large uncertainty in the designing of optimum acquisition parameters (Coman et al. 2005). Usually, acquiring high-fold 3D seismic surveying would not be feasible in such circumstances. The solution on the one hand is to use interpolation and regularization of land data to make it as close to a regular grid and on the other hand, a processing tool is used that could make acceptable subsurface image in low fold and not regular distributed data.

The common reflection surface (CRS) method was introduced as a macro velocity model independent technique in literature of seismic imaging (Hubral, 1999). The CRS processing can provide enhanced seismic images of sparse 2D and 3D data. In 3D seismic data processing, the CRS technique has also increasingly been established as a comprehensive tool covering the whole processing range from pre-processing and subsurface imaging up to the reservoir characterization. Another use of the 3D CRS processing method is to provide appropriate acceptable subsurface coverage even in low-fold data. Conventional methods increase the subsurface illumination in low fold data by coarsening the bin size (Gierse et al. 2009). Other benefits of the CRS method in seismic exploration have been demonstrated in

several projects (Pruessmann et al. 2012).

Seismic image obtained by the CRS technique allows increasing the signal content on the wavelet and thus getting a clearer image of the subsurface structures (Eisenberg-Klein et al. 2008). In case of sparse data and existing gaps in data due to surface mutes or missing common midpoint (CMP) traces, the CRS processing automatically closes these gaps by dip-consistent interpolation and extrapolation of seismic data (Gierse et al. 2009; Höcht et al. 2009).

The CRS stack method considers the location, the local orientation and the curvature of the reflector in the subsurface by introducing three kinematic wavefield attributes (Mann, 2002). Conventional processing chain mostly analyze individual CMP gathers and eliminate offset dependency of reflection events to obtain a zero offset (ZO) image of the subsurface structures (Vafidis et al., 2012). Compared to the conventional CMP method, the number of contributing traces into stacking is dramatically increased in the CRS stack method. This will result in improving signal to noise ratio (S/N) and better quality of the final seismic image (Zhang et. al., 2001). In the CRS literature, the fold number is equal to the number of traces falls into the stacking surface. This surface and fold number are based on the shape of the CRS stacking operator, which is spread over several CMP locations according to the stacking aperture. Shape of the CRS stacking surface is related to three CRS kinematic wavefield attributes. The shape and the size of this surface should be defined in a way to increase coverage and spatial regularization (fundamental to any pre-stack migration process based on offsets plans).

Jäger (1999) showed that the kinematic wavefield attributes of that surface could be approximated for limited offsets and limited mid-point apertures by a parameterized function of distance to the normal ray emergence point and half-offset by:

$$t_{\text{hyp}}^2(x_m, h) = \left[t_0 + \frac{2\sin\alpha(x_m - x_0)}{v_0} \right]^2 + \frac{2t_0\cos^2\alpha}{v_0}\left[\frac{(x_m - x_0)^2}{R_N} + \frac{h^2}{R_{\text{NIP}}} \right] \quad (1)$$

Here, α is the emergence angle of normal ray to the surface, R_N is the radius of the wave front curvature of a hypothetic normal wave and R_{NIP} is the radius of wave front curvature of hypothetical normal-incidence-point (NIP) wave, v_0 is the surface velocity and h is the half-offset. The parameters α, R_N, and R_{NIP} are called CRS kinematic wavefield attributes. During the CRS stack process, optimum values for these parameters are automatically determined independently for each zero offset sample. This is realized by varying three parameters (α, R_N, R_{NIP}) and performing a coherency analysis along the stacking operator in the multi-coverage data. The critical parameter in this technique is the CRS aperture in mid-point and offset direction. Large CRS aperture will introduce more random noise into stacking, which compromises the lateral resolution. Small aperture prevents exact surface calculation of travel times and accordingly results to a poor positioning of the reflection elements (Battaglia, 2013). Therefore, determination of the CRS stacking aperture is an important parameter while the CRS method would be used for filling the gaps in acquisition by trace interpolation. Sui et al., (2009) proved that defining proper aperture in the CRS method, could dramatically improve quality and resolution of the final depth image.

2. The CRS interpolation and acquisition design

Existence of large gaps in acquired seismic data due to various obstacles on land and/or severe marine currents would heavily impact the economic of the survey and consequently final image of the subsurface (Yang and Gao, 2015).

While modern anti-multiple techniques require high density of sources in acquisition, (which is simply too costly to achieve), offset-azimuth regularization optimization should be considered as the priority to increase subsurface coverage required any seismic imaging method (Spitz, 1991; yang et al., 2013). Source-receiver regularization, on the contrary, optimizes the surface coverage by regular acquisition geometry. This provides a regular distribution of input data for migration in the shot domain, but does not fully normalize the subsurface fold. However, even when there is no gap in the data, irregularly positioned traces would provide unpleasant consequences when the processing

algorithms require a regular sampling.

This problem also shows up in merging and regularization of vintage 3D seismic data with various acquisition designs. Incompatible binning grids due to different acquisition parameters also lead to large portions of empty grid cells after regrinding. To obtain a final high resolution seismic image, it is required that these effects are corrected by applying various processing techniques.

Chira-Oliva et al., (2005) presented a modified 2D ZO CRS stack method to consider effects due to hard topography. By means of this new CRS formulation, they obtain a high resolution ZO seismic section, without applying static corrections. The residual static corrections also may be evaluated from the kinematic wavefield information derived from the CRS stack process through the so-called CRS-based residual static correction method (Koglin et al., 2006). Since number of traces falling into the CRS-supergather can significantly increase according to the number of traces belonging to one CMP gather, thus number of contributing cross-correlation results would be generally much larger than provided by conventional CMP-based residual static correction methods. This will result in higher illumination of the subsurface target and/or filling the gaps might be provided in acquisition step (Liu et al., 2015).

Gierse et al., (2006) also introduced CRS parameter definition ability for static correction in hard topography land seismic data. They have used benefit from the large CRS stacking aperture and large fold number which increases number of estimates for single static shifts. The large CRS stacking fold also increases the S/R ratio in the final CRS stack section.

With the CRS technique, it is possible to reconstruct missing traces in a seismic data by mapping seismic event data along the CRS traveltime surfaces. Cardone et al., (2003) used 3D ZO CRS method for imaging narrow azimuth data. In their formulation, once the emergence and azimuth angle of the normal ray has been derived, the elliptical azimuthal dependency of the NMO velocity could be estimated. This strategy works even if seismic traces are concentrated along a special predominant azimuthal direction. Andrade et al., (2005) introduced a particular interpolation method to reconstruct traces in gaps on a regular grid. Their method was defined in the CRS framework and is a model independent technique. Since the required kinematical parameters are computed directly from the data in this strategy, amplitudes of the reconstructed traces are simply interpolated from present data. The CRS stack method also could be used as a suitable tool for regularizing CMP and offset coverage within a single 3D seismic datasets (Gierse et al., 2009). Trad (2009) introduced a five dimensional (5D) simultaneous algorithm to use information from a well sampled dimension to infill the other poorly sampled dimension in a data cube. This strategy also could be used to deal with large gaps and sparseness in seismic data more effectively. Method of Trad (2009) utilizes a Fourier reconstruction approach which provides high-fidelity data reconstruction to reduce spatial sampling problems, increase fold and improve the offset-azimuth distribution of data. This method was later successfully used by Poole (2010) as an anti-leakage Fourier transform as a 5D reconstruction in seismic data.

In this study, we combined the interpolation method introduced by Andrade et al. (2005) with the strategy of Trad (2009) here to fill the gaps in a seismic acquisition in oil filed in SW of Iran and change the acquisition parameters. Subsequently these interpolated traces were distributed to bins to obtain a regular trace distribution. The interpolation idea used here consists of using a local second order approximation for describing one wave front of the reflection events. Additionally, local dips as well as local curvatures of reflection event are taken into account. For one sample t_c of an interpolated trace located in this data cube, a local iso-phase surface is described by a second-order approximation:

$$t_c(\Delta x, \Delta h) = t_c + b_0\Delta x + b_1\Delta h + a_{00}\Delta x^2 + a_{01}\Delta x\Delta h + a_{11}\Delta h^2 \qquad (2)$$

Where $\Delta x = (x - x_c)$ and $\Delta h = (h - h_c)$ are the midpoint/shot and the offset relative coordinate, respectively. Parameters b_0 and b_1 represent local dips in midpoint/shot gather and offset direction, respectively. The second-order derivatives, a_{00}, a_{01} and a_{11}

determine the local curvatures of a reflection event together with the dips b_0 and b_1. These parameters could also be related to the wavefront curvatures and/or reflection curvature. Howsoever equation (2) would be used to interpolate seismic traces at an arbitrary position and fill the possible gapes that might exist in any 3D data acquisition. However, to interpolate any desired seismic trace by equation (2), firstly the kinematic wavefield attributes would be interpolated from the parameters on the search grid. Using the interpolated parameters, a stacking surface in time domain using equation (2) would construct and subsequently computes the output trace by stacking the data along the predefined surface. Figure 1a illustrates the proposed interpolation procedure in offset and midpoint direction, whilst green trace is interpolated by red traces in offset and midpoint direction. Figure 1b shows the final CRS stacking related surface used for trace interpolation. Some conventional interpolation approaches fails to use

advanced multi-dimensional interpolation and regularization techniques which can play a pivotal role in improving quality of seismic images. Since the interpolation strategy introduced here considers wide azimuth geometry, therefore it is able to use new advances in multi-dimensional interpolation techniques.

The CRS interpolation strategy also uses more information of reflector from several sets of traces in midpoint and offset directions, (conventional methods only use a group of traces in a CMP gather for trace interpolation), and therefore it could reconstruct seismic trace satisfactory close to real trace. Figure 2 shows an example of comparison between CRS trace interpolation and conventional *f-x* trace interpolation method for an arbitrary trace. As it could be seen, both methods could reconstruct the missed trace by interpolation. However, amplitude spectrum of the reconstructed trace by the CRS method could better recover frequency content of the original trace.
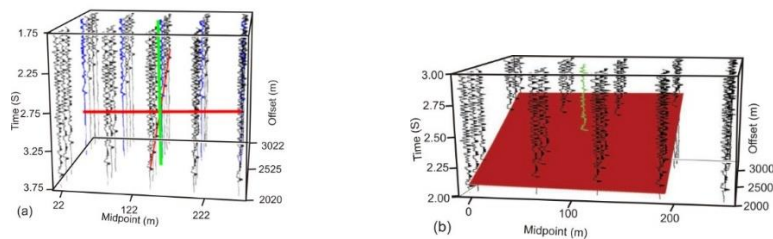

Figure 1. (a) Interpolation scheme, parameters search along offset and CMP directions (red line) to calculate the desired trace (green line) and (b) Interpolation in a 3D data space (t, x, y), (Andrade et al. 2005).
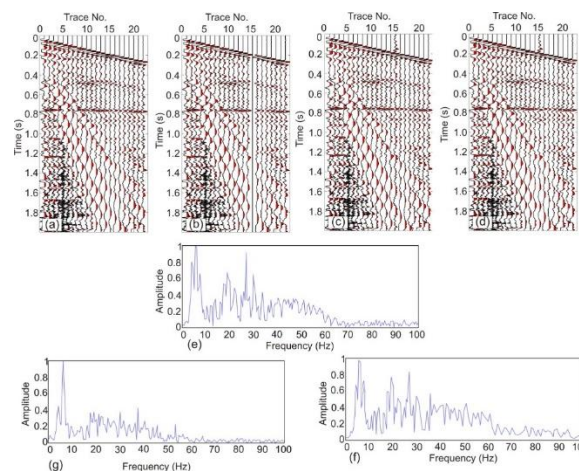

Figure 2. (a) A shot gather sample of a real raw field data with 22 traces and 2s of recording time. (b) Trace number 15 is removed and intended to be constructed. (c) Reconstruction of the missed trace by the *f-x* interpolation method (d) Reconstruction of the missed trace by the CRS trace interpolation method (e) Amplitude spectrum of the real trace number 15 (f) Amplitude spectrum of the reconstructed trace by the f-x trace interpolation method and (g) Amplitude spectrum of the reconstructed trace by the CRS trace interpolation method.

3. The study field designing parameters

The study area is situated in SW of Iran near the city of Ahwaz, approximately 60 *km* long by 15 *km* wide, (Figure 3). A river also follows near the southeast boundaries of the study area. Most part of the land in study area is covered by aeolian sand and alluvial varying from a thin layer to sand dunes rising to a thick of 40 *m*. The lower lying areas, especially close to the river, are heavily cultivated while many irrigation ditches and larger concrete lined canals cross them. The other obstacle is a long rocky ridge which runs through the north central part of the prospect. Some parts of the study area in the north bank of the river were classified as a battlefield area and needed mine clearance before any operations could commence. All these obstacles would provide lots of gaps in seismic acquisition design that should be compensated by any trace interpolation or fold increasing coverage techniques. The related target is an anticline elongated with NW-SE trend, which is the primary aim, suppose that it defines orientation of shot and receiver lines.

The main objective of this study is to design a proper 3D seismic acquisition geometry using CRS interpolation ability to fill the gaps. An old 2D seismic survey available from this area was also used for testing the CRS parameters and attributes to have a primary guess of acquisition designing parameters.

3.1. Geological description

The structural framework of the target anticline was previously built by combination of 2D seismic information and well logs available from three wells in the area. However, to have better image of the target formations, the old 2D lines were processed by the CRS method to obtain depth contour map of the target formations. Figure 4 illustrates 2D processed lines by the CRS method and the structural contour map of the anticline with location of two 2D seismic lines (bold red lines) on it. As it could be seen on the interpreted seismic lines in figure 4, anticline depicts steep dips on its flanks, which necessitate considering large aperture both in acquisition and in imaging steps. However, there is a small difference in the concept of apertures used by the CRS method and migration aperture used by any migration algorithm (Höcht et al., 2009). Figure 5a shows difference between these two apertures.

The other important parameter used in equation (1) in the CRS parameter is the near surface velocity, v_0. This parameter is used to estimate the location of the hypothetical source point of the NIP wave and normal wave in the CRS method, shown in Figure 5b. Again it should be noted that any desired migration algorithm uses a linear velocity model, which is different with constant surface velocity used in the CRS. For an aribtary reflection point S_{NIP}, circular approximations of the wavefronts of the NIP wave and the normal wave are depicted in Figure 5b. Geometrically, apparent location of the NIP wavefront source stem from the object point S_{NIP}, shown by S^*_{NIP} as the center of NIP curvature. S_N also denotes the center of curvature of the reflector segment. With corresponding image point by S^*_N it could be shown that the hypothetical reflector segment at S^*_{NIP} would yield the same emergence angle α and radii of curvature R_N and R_{NIP} at x_0 for a homogeneous model with near surface velocity of v_0. Thus the acquisition should be designed in way that the CRS aperture could contain information from steep dips and point source location, S^*_{NIP} and S^*_N, of the target formation. Therefore, concept of the CRS aperture was used for maximum offset design.

After defining the aperture based on the maximum dip of the target formation in the study area, the underground contour map of it should also be defined for final bin size calculation. Information of the top formation elevation from well data was overlaid on seismic result to perform well – seismic tie process. Afterwards accurate depths of horizons have been defined for target formations. To remove structural errors inherent in time migration, it is necessary to convert time-migrated images into the depth domain. This procedure could be performed either by migrating the original data with a pre-stack depth migration algorithm or by depth migrating post-stack data after the time de-migration (Cameron et. al. 2008). The obtained depth contour map of the target formation from previously depth migrated data are illustrated in figure 6. The velocity model used for depth migration was obtained by the stereo tomography method, which uses the CRS attributes for velocity model building (Panea et al. 2005). The counter depth map of the target formations illustrates elongation of the anticline; its closure and the possible maximum offset could be designed by considering the CRS aperture.
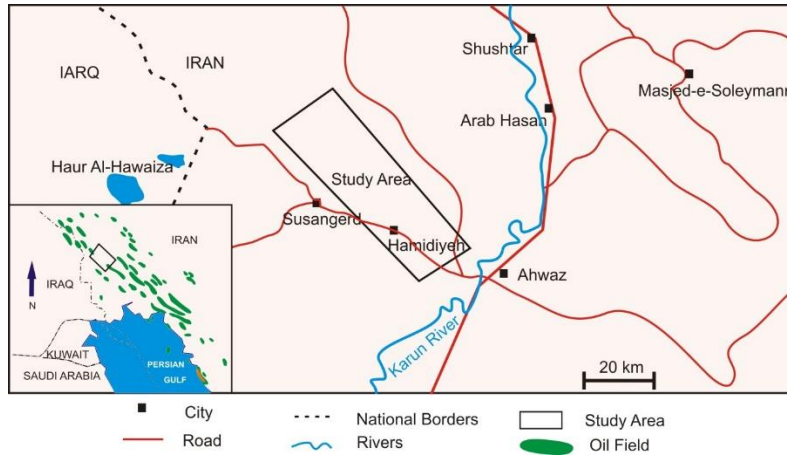
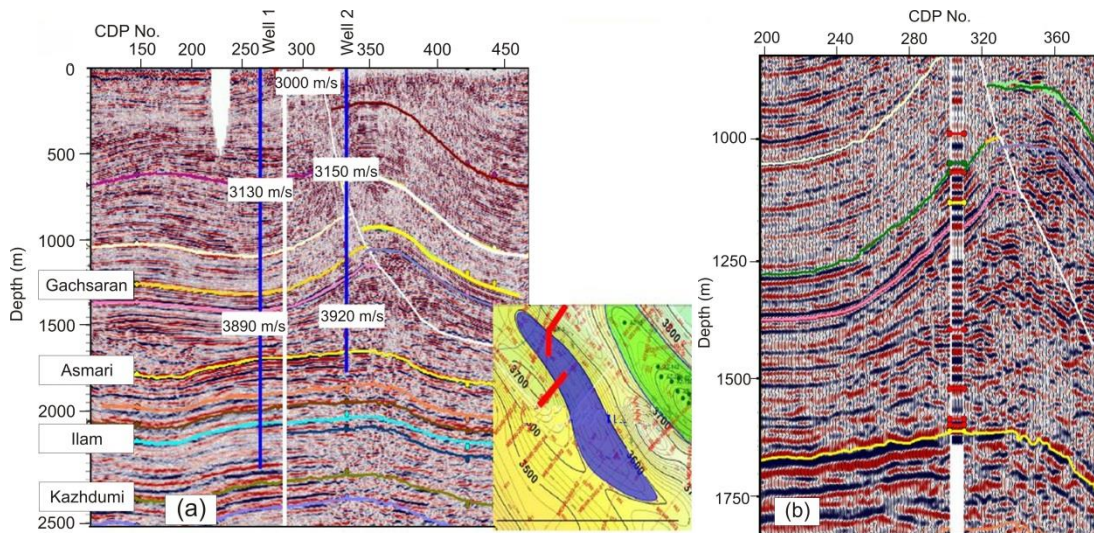**Figure 3.** Location and the boundary of the study area

Figure 4. Time migration section on the CRS stacked data, The middle figure shows location of the seismic lines on the target anticline. (a) Faulted anticline with steep dips and (b) steep dips layer beneath the fault
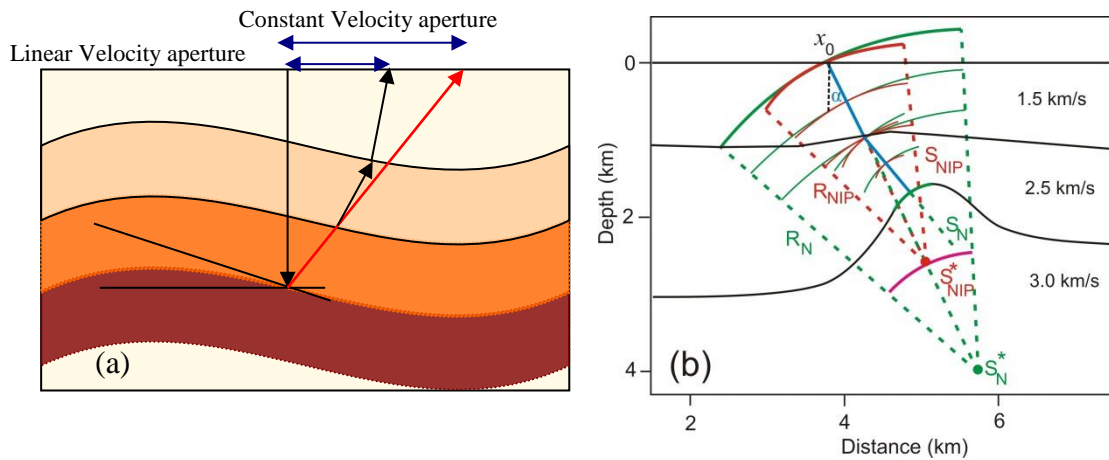

Figure 5. (a) Comparison of the CRS aperture with constant velocity and migration aperture with linear velocity. (b) The NIP wave (red), the normal wave (green) and the ZO ray (blue) are shown. The apparent source of the NIP wavefront is S∗NIP and S*N for normal wave. The hypothetical reflector segment at S∗NIP (magenta) would yield the same emergence angle α and radii of curvature R_N and R_{NIP} at x_0 for a homogeneous model with velocity v_0 (Mann, 2002).
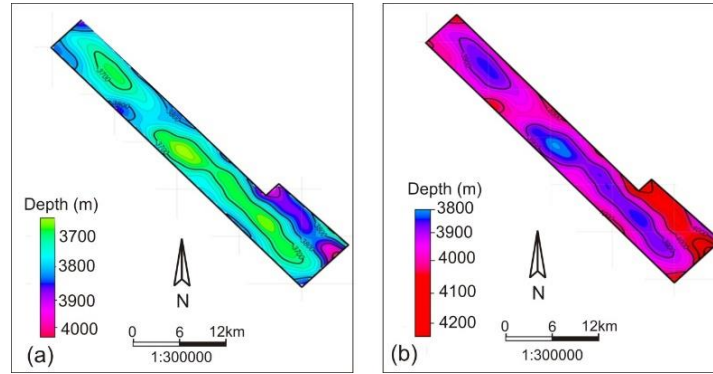
Figure 6. Depth map of two formation target, (a) Ilam formation and (b) Sarvak formation
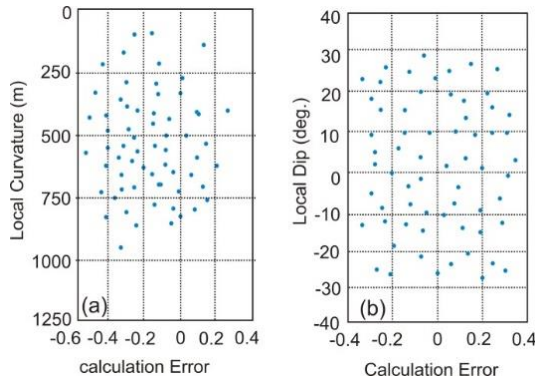

Figure 7. (a) Curvature and (b) dip of two-target reflector defined by search in seismic data in common shot and common offset domain, respectively.

3.2. Bin size and maximum offset calculation

CRS parameter search for defining the stacking surface for trace interpolation is the first step in the proposed strategy. Kinematic wavefield attributes shown by parameters in equation (2) are related to the local curvature and local dip of reflectors. These parameters are defined in two search steps by searching in two subdomains of seismic data. Local curvatures of reflectors in different segments are defined by searching in common shot data and local dip is defined by search in common offset domain. These segments are shown by bold green line on the subsurface layer in figure 5b. The parameters R_{NIP} and α (figure 5b) define local curvature and dip of the reflector (bold green segment). For each target formation, these parameters could be defined and evaluated further by coherency analysis. Figure 7 shows curvature and dip estimation (parameters of equation (2)) with calculated errors for the two target formation in the study area. Curvatures of reflectors in figure 6 are shown by radius of curvature and sign in dip

parameter that shows dip orientation.

The next steps are bin size analysis followed by trace interpolation and distribution steps. In 3D seismic acquisition design, the bin calculation should be designed in such a way to reduce spatial aliasing in the recorded data and prevent dip aliasing in steep dip layers. Three different strategies were used for bin size analysis in this study. These strategies use the following equations:

$$B = \frac{V_{ave}}{4 \times f_{dom} \times \sin\theta} \tag{3}$$

$$B = \frac{V_{int}}{4 \times f_{max} \times \sin\theta} \tag{4}$$

$$B = \frac{V_{int}}{N \times f_{dom}} \tag{5}$$

Result of the bin size analysis according to those three strategies for the target formation is shown in tables 1-3. Usually the smallest bin size for each target formation is selected as the final designing parameter. This is also near (with slight difference which is negligible) the bin size value for the Sarvak formation base on the dip versus bin size analysis shown in figure 7. The other parameter, which is the maximum offset, is proportional to patch size. The larger the maximum offset, the larger the patch dimensions. According to the CRS aperture, depth and maximum dip of the target formation, maximum offset was designed as about 5000 *m*. This not only covers the maximum depth, (4700 *m*), but also is larger than the CRS aperture used for 2D CRS stack (3500 *m*). Defining the largest possible value for minimum offset is based on the shallowest target in the area. In this study, the shallowest target achieved at 500 *m*. Consequently, 500 *m* is the best value for largest possible value for minimum offset.

Orientation of the structure shows a 130 degree of the long axis with the NW-SE direction. Consequently, the best fit of design geometry is to put the receiver lines perpendicular to the long axis of the structure, which is namely here 40 degree. Therefore, by supposing a rectangular design, source line inclination should be designed to be 130 degree. Finally, the acquisition parameters are shown in table 4.

Table 1. Bin size relations to bin calculation with equation (3)

Target formation	V_{ave} (m/s)	f_{dom}	Max.dip(θ)	Bin Size (m)
Asmari	3290	40	30	41
Ilam	3491	40	30	43
Sarvak	3621	40	50	30

Table 2. Bin size relations to bin calculation with equation (4)

Target formation	Vave (m/s)	fmax	Max.dip(θ)	Bin Size(m)
Asmari	4408	50	30	44
Ilam	5285	50	30	52
Sarvak	4353	50	50	28

Table 3. Bin size relations to bin calculation with equation (5)

Target formation	Vave (m/s)	fdom	N	Bin Size(m)
Asmari	4408	40	4	27
Ilam	5285	40	4	33
Sarvak	4353	40	4	27

Table 4. acquisition parameters proposed for 3D seismic acquisition.

Patch parameters

parameter	Value	Parameter	Value
Live Channels	2400	Receiver line Bearing (azimuth)	40
No. of Receiver line	12	Roll Inline/Crossline	360/1080m
Active channel per line	200	In-line fold taper	1800
Receiver interval	40	Receiver density per sqkm	69
Receiver line interval	360	Source point interval	40
Source points per Salvo	27	Source line direction	Orthogonal
Source line interval	400	Source Line Bearing (azimuth)	130
Cross-line fold taper	900	Patch Length (m)	7960
Source density per sqkm	62.4	Patch Width (m)	3960

Geophysical attributes parameters

parameter	Value	Parameter	Value
Bin size	20×20 m	Largest minimum offset (m)	509.9
In-line fold	10	Inline maximum offset (m)	3980
Cross-line fold	6	Cross-line maximum offset (m)	2180
Nominal fold	60	Maximum offset (m)	4710
Minimum offset (m)	28.28	Surface Full Fold before migration (Sq.Km)	683

Statistics parameters

parameter	Value	Parameter	Value
Total number of source lines	58	Surface Acquisition operation area (Sq.Km)	875
Total Sources	54594	Total Operating Length of Shot lines(km)	2245
Total number of receiver lines	157	Total number of receiver stations	59730
Aspect Ratio (%)	49.7	Total Length of Receiver Lines(km)	2186

Although only seismic data related to the full fold area is considered as final acquired data, however, the edge management should be performed to reduce cost and width of non-full fold area. The edge management procedure consists of two section; migration aperture consideration and fold taper design. The former is independent on design approach and is directly being affected by situation of structure boundary (image area) and geometrical properties and also depth of formation bellow the boundary area. However, the fold taper is only related to design parameters and patch size. Figures 8a shows result of the fold analysis which is the final fold distribution in the area. As it could be seen, the target formation is completely covered by the full fold area in this design. Figure 8b also shows bin number versus azimuth for a part of the full fold area. This figure shows redundancy of acquired data in each bin. The more redundancy in each bin depicts higher illumination of the target formation. Redundancy value for most part of the area is 1, which shows possible illumination loss in the case of small gaps in acquisition due to field obstacles. The higher redundancy will reduce losing illumination in case of field obstacles and possible gaps in data acquisition. Figure 10 also shows the rose diagram and offset distribution in different azimuths.

As it could be seen in both Figures 10a, some bins in some azimuths are not fully filed by traces. In this case, bins in NW-SE trend are not full fold, while bins in NW-SW trend are covered by full fold (red cells). Figure 10b shows offset distribution in each azimuth. Obviously small offset in each azimuth is directly related to reducing fold coverage in those directions. Thus after binning procedure, bins with less number of traces should be fulfilled with interpolated traces. Therefore seismic traces were interpolated in gaps area by the CRS method and then these traces were distributed throughout the empty bins. For distributing traces, distribution method introduced by Trad (2009) was used for allocating interpolated traces to selected bins. Each interpolated traces in any arbitrary swath have been partitioned into two data sets according to the following rule:

1. If only one trace appears in one bin and in one offset class, that trace is copied in two data sets,

2. If several traces are present in one bin and in one offset class, that trace with the closest azimuth is copied in one data set, and the interpolated trace with the farthest azimuth is added to the other data set.

After applying this method, there was no emptier bin in the data. Figure 11 shows distribution of traces in different offsets before and after applying CRS interpolation and trace distribution on the pre-stack data. Figure 11b shows the increase in trace count for each offset after trace interpolation. Figure 12 shows redundancy of traces in different azimuths before and after applying CRS interpolation and trace distribution. As it could be seen in figure 12b, redundancy is increased in more bins comparing before interpolation procedure in figure 12a. Increasing redundancy in bins will reduce risk of empty bins or low illumination of the target formation in the case of acquisition obstacles.
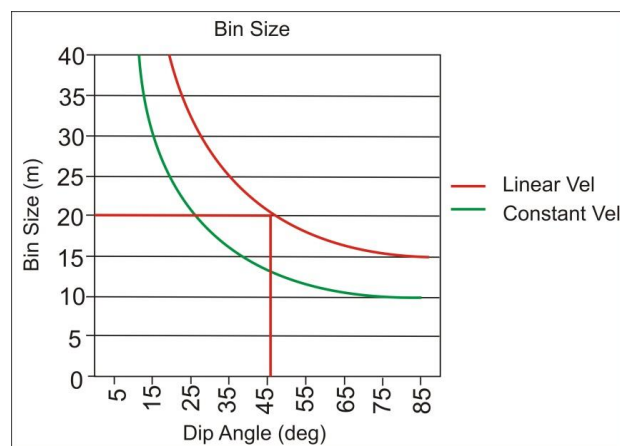

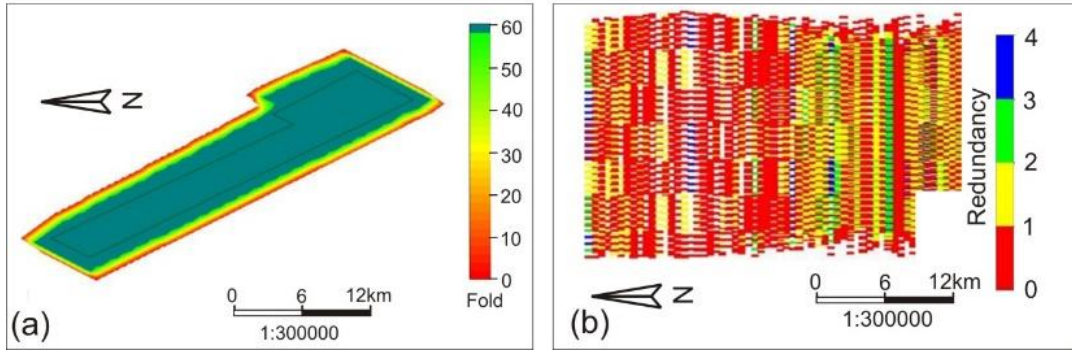**Figure 8.** Dip angle versus bin size chart, and bin calculation (Based on Sarvak information)

Figure 9. (a) Fold distribution display and (b) Bin number versus Azimuth
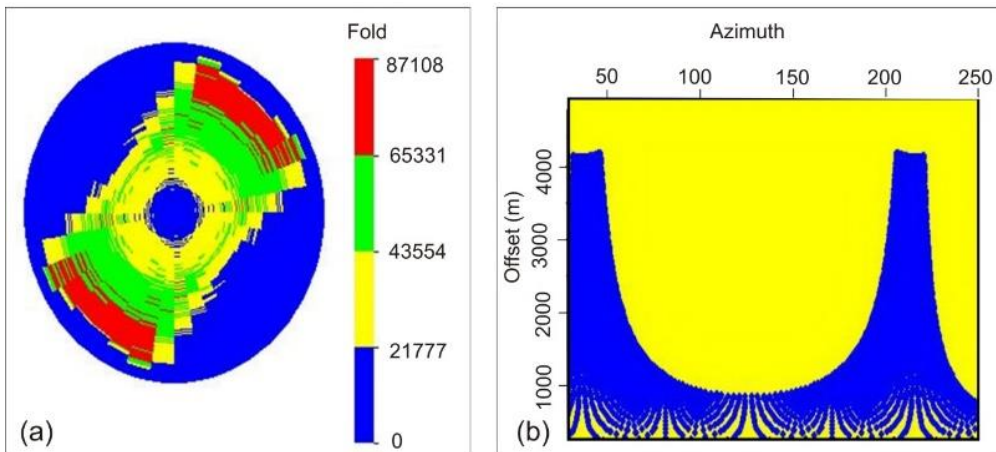

Figure 10. (a) Rose diagram and (b) Azimuth versus Offset diagram that shows distribution of offset in each azimuth.
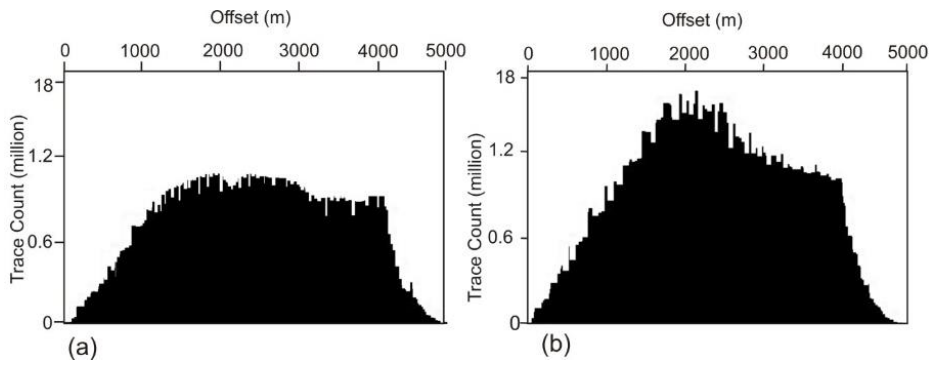

Figure 11. (a) Trace distribution on the offsets before trace interpolation and (b) after applying CRS interpolation and trace distribution
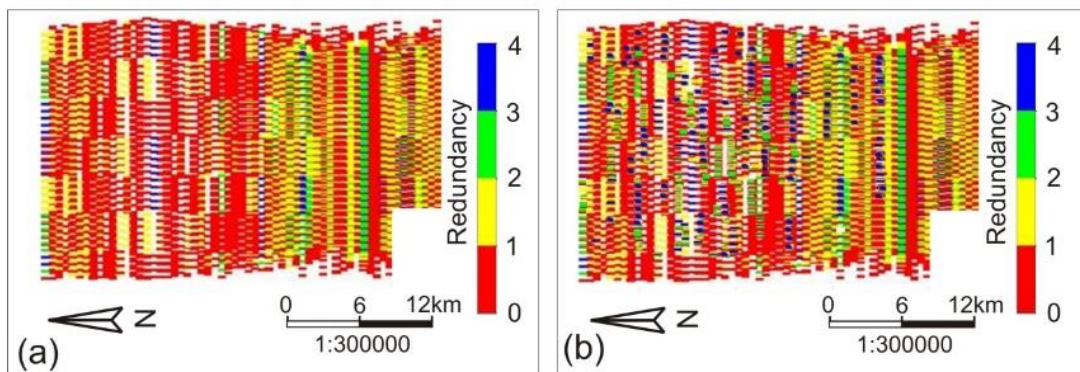

Figure 12. Bin number versus azimuth (a) before and (b) after applying CRS interpolation and trace distribution

4. Conclusion

Seismic trace interpolation and trace distribution methods could come to assist inevitable irregularities in acquisition and make normal dispersion of trace coverage in the area. The CRS method is an appropriate technique for this purpose. In this study, trace interpolation ability of the CRS method was combined with an appropriate distribution tool to increase fold in each azimuth in a 3D seismic data acquisition design in SW of Iran. Searching for optimized CRS imaging parameters or kinematic wavefield attributes on the old 2D seismic lines from the study area was performed for appropriate initial acquisition parameter estimation. These parameters were used for initial value definition for parameters of maximum offset and bin size. These parameters were used for acquisition geometry design in three scenarios. Thereafter bin size analysis was performed for the target formation and optimum bin size was selected for the acquisition design.

However, the most important point in this study was increasing the nominal fold, increasing normal distribution of fold in all azimuths and increasing normal distribution of traces in each bin. Results showed that by applying a combination strategy of two appropriate methods for trace interpolation and trace distribution, they were successful to achieve the already defined objects. The interpolation ability of the CRS method was used here that proved this technique could be considered as an alternative for trace interpolation, and increasing fold in gaps of acquired data. This is a great advantage for further processing to increase illumination of the target area and obtain a high resolution image of the subsurface structures. The proposed design for the study area could be considered as the optimized design that could be expected to have adequate nominal fold and source- receiver density.

References

Andrade, L., Höcht, G., Landa, E. and Spitz, S., 2005, QC of a marine seismic trace reconstruction technique, SEG annual meeting, Huston, USA.

Battaglia, E., 2013, Seismic refection imaging of near surface structures using the common refection surface (CRS) stack method, Ph.D. dissertation, University of Cagliari, Italy.

Cameron, M., Fomel, S. and Sethian, J., 2008, Time-to-depth conversion and seismic velocity estimation using time-migration velocity, Geophysics, 73, 205-210.

Chen, Y., Huang, W., Zhang, D. and Chen, W., 2016, An open-source Matlab code package for improved rank-reduction 3D seismic data denoising and reconstruction, Computers & Geosciences, published online, doi: 10.1016/j.cageo.2016.06.017.

Chira-Oliva1, P., Cruz, J. C. R., Garabito, G., Hubral, P. and Tygel, M., 2005, 2D ZO CRS stack by considering an acquisition line with smooth topography, Revista Brasileira de Geofisica, 23(1), 15-25.

Cardone, G., Cristini, A., Marchetti, P., Zambonini, R., Hubral, P. and Mann, J., 2003, 3D zero offset CRS stack for narrow azimuth data: formulation and examples, EAGE/SEG Research Workshop, Trieste, Italy.

Coman, R., Gierse, G., Trappe, H., Robinson, S., Owens, M. and Nielsen, E. M., 2005, CRS seismic processing, A new approach to obtain high-resolution images from sparse 3D-exploration surveys, International Petroleum Technology Conference, Doha, Qatar.

Eisenberg-Klein, G., Pruessmann, J., Gierse, G. and Trappe, H., 2008, Noise reduction in 2D and 3D seismic imaging by the CRS method, The Leading Edge, 27(2), 258-265.

Gierse, G., Pruessmann, J. and Coman, R., 2006, CRS strategies for solving severe static and imaging issues in seismic data from Saudi Arabia., Geophysical Prospecting, 54(6), 709-719.

Gierse, G., Trappe, H., Pruessmann, J., Eisenberg-Klein, G., Lynch, J. and Clark, D., 2009, Enhanced velocity analysis, binning, gap infill, and imaging of sparse 2D/3D seismic data by CRS techniques, SEG Annual Meeting, Houston, Texas.

Höcht, G., Ricarte, P., Bergler, S. and Landa, E., 2009, Operator oriented CRS interpolation, Geophysical Prospecting, 57, 957-979.

Hubral, P., 1999, Macro-model independent seismic reflection imaging, Journal of Applied Geophysics, 42, special issue.

Jäger, R., 1999, The common reflection surface stack: theory and application, Diploma thesis, University of Karlsruhe.

Kim, B., Jeong, S. and Byun, J., 2015, Trace interpolation for irregularly sampled seismic data using curvelet-transform-based projection onto convex sets algorithm in the frequency–wavenumber domain, Journal of Applied Geophysics, 118, 1-14, doi: 10.1016/j.jappgeo.2015.04.007.

Koglin, I., Mann, J. and Heilmann, Z., 2006, CRS-stack-based residual static correction, Geophysics, 54, 697-707.

Liu, W., Cao, S., Li, G. and He, Y., 2015, Reconstruction of seismic data with missing traces based on local random sampling and curvelet transform, Journal of Applied Geophysics, 115, 129-139, doi: 10.1016/j.jappgeo.2015.02.009.

Mann, J., 2002, Extensions and applications of the common-reflection-surface stack method, Ph.D. thesis, University of Karlsruhe.

Panea, I., Landa, E., Drijkoningen, G.G. and Baina, R., 2005, Improvement of seismic imaging in a low signal-to-noise area by the use of post-stack stereotomography, Journal of Balkan geophysical society, 18(4), 161-174.

Poole, G., 2010, 5D data reconstruction using the anti-leakage Fourier transform, 72nd EAGE Conference and Exhibition, Expanded abstracts, B046.

Pruessmann, J., Bergmann, P., Gierse, G., Lippmann, A. and Lüth, S., 2012, CRS workflow for improved seismic resolution and monitoring of the Ketzin storage site, 74th EAGE Conference and Exhibition, workshops.

Spitz, S., 1991, Seismic trace interpolation in the F-X domain, Geophysics, 56(6), 785-794. doi: 10. 1190/1.1443096

Sui, F., Li, Z., Sun, X., Li, F. and Li, D., 2009, Successful application of optimized aperture based CRS stack in the Shengli exploration area, Applied geophysics, 6, 377-383.

Trad, D., 2009, Five-dimensional interpolation: recovering from acquisition constraints, Geophysics, 74, 123-135.

Vafidis, A., Andronikidis, N., Economou, N., Panagopoulos, G., Zelilidis, A. and MManoutsoglou, E., 2012, Reprocessing and interpretation of seismic reflection data at Messara Basin, Crete, Greece, Journal of the Balkan geophysical society, 15(2) 31-40.

Yang, P. and Gao, J., 2015, Enhanced irregular seismic interpolation using approximate shrinkage operator and Fourier redundancy, Journal of Applied Geophysics, 116, 43-50, doi: 10.1016/j.jappgeo.2015.02.007.

Yang, P., Gao, J. and Chen, W., 2013, On analysis-based two-step interpolation methods for randomly sampled seismic data, Computers & Geosciences, 51, 449-461, doi: 10.1016/j.cageo.2012.07.023.

Zhang, Y., Bergler, S. and Hubral, P., 2001, Common-reflection-surface (CRS) stack for common offset, Geophysical Prospecting, 49, 709-718.